In situ metallic porous structure formation due to ultra high heating and cooling rates during an electromagnetic pulse welding

T. Sapanathan[1, *], R.N. Raoelison[1, 2], N. Buiron[1] and M. Rachik[1]

[1] *Sorbonne universités, Université de technologie de Compiègne, laboratoire Roberval, CNRS UMR - 7337, Centre de recherche Royallieu, CS 60319, 60203 Compiègne cedex, France*
[2] *Université de Bourgogne Franche Comté, Université de Technologie de Belfort Montbéliard, IRTES - EA7274, 90100 Belfort, France*

*Corresponding author: Thaneshan Sapanathan (email: thaneshan.sapanathan@utc.fr)

Abstract

Porous structure formation resulted at the interface of electromagnetic pulse welded joints are investigated and revealed, to identify the development of sub-micron to few micron sized pores due to ultra high rate of heating and cooling. Collision velocity along the overlapping length was predicted using a multi-physics numerical simulation and subsequently this velocity field was used to estimate the heating and cooling rates as about 10^9 °Cs^{-1}. Predicted temperature, pressure and strain variations clearly evidence the observations of porous structure formation that is potentially facilitated by sequential phenomena of pores nucleation, coalescence and growth within the molten intermediate phase.

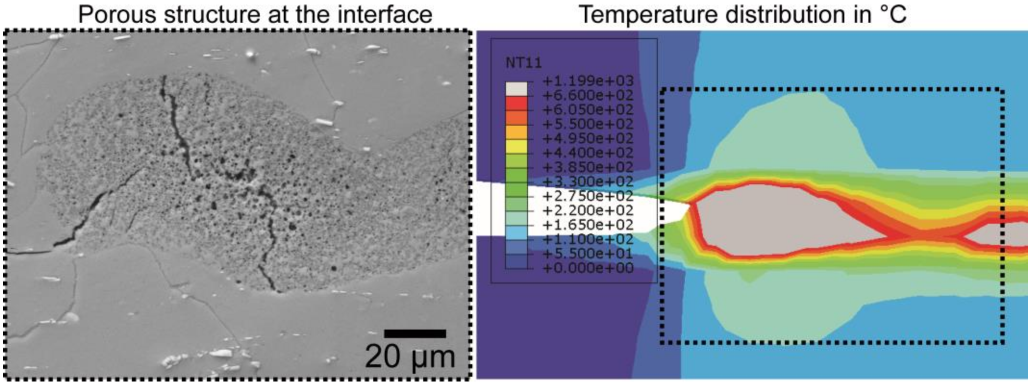

Graphical Abstract

Keywords: high speed impact; pores; interface; thermomechanical effect, ultra high heating

Nanoporous structures have multiple applications in various fields while their fabrication methods are very limited [1]. Therefore, exploring the formation of porous structure is helped to understand the underlying physics of the phenomena that could lead to identify a potential method to produce the porous nature within a hybrid part or in bulk quantities. Therein, this study investigates an observation of porous structure formation at the interface of electromagnetic pulse welded joint and revealing an understanding of its prevalent mechanism.

During an electromagnetic pulse welding (EMPW), the welding occurs with a high impact velocity when the work pieces experience a strain rate of up to $10^2 – 10^4$ s^{-1} [2], and the interface may undergoes an incredibly high strain rate of up to $10^6 – 10^7$ s^{-1} [3]. Although, it is theoretically possible to produce the velocity of up to 15000 m/s during an EMPW, the velocity is limited to be used below 1000 m/s in practice, because of the durability of the coil and power requirements [4]. It has been reported that the impact velocity during the welding is in the range of 200-400 m/s [2, 3], while an impact velocity of 350m/s produces a regular zigzag wave at the interface for a steel-aluminum joint [5]. Various interfacial phenomena, viz., vortex formation, interfacial shearing, wave formation, jetting and ejection are also observed as a consequence of the high impact velocity during the welding process [6-8].

Although, earlier studies reported about the formation of porous structure at the interface during an EMPW, there was particularly no attention given to the physical phenomena and characterization or formation of the porous interface [8-12]. This could be mainly because of the EMPW's nature that has generally been known as a cold welding, is in contradiction with a prevalent mechanism to bring the favorable condition for the porous structure formation [13-15]. However, the high velocity impact causes a large dissipation of plastic energy leading to significant localized heating at the vicinity of the interface [16-18]. Moreover, recent findings support the hypothesis of the localized interfacial heating and report the consequential effects of ultrafine grains formation [19], interfacial melting [6, 17], evidence of molten metallic flow [6], formation of intermetallic compounds [19-21], nanoscale amorphization of interface and grain boundary [21, 22] and development of columnar grain structure at the interface [23].

The observation of pores' nucleation at the interface could also be interpreted as a result of dissolved gases at the high speed, thereby trapped gases nucleate into bubbles and grow with the rapid cooling of the molten mass, as observed during an impact and rapid solidification experiment [1]. Nevertheless, one could be immediately ruled out the phenomenon of dissolving gases in the local interface region because of the high speed nature with the materials' jetting that facilitates to escape the gases from the impact region. However, it has been identified that the surrounding gaseous environment affects the emitting light of the jet and the pressure wave during the impact [24]. Moreover, the jetting materials could consist of parent metals and those oxides [24-27], these observations allow claiming for an occurrence of interaction between the surrounding gases and metal substrates at the interface.

Nevertheless, various heating sources contribute to the local heating suggest that the fast compression of the gases and the ejection of jet at a supersonic speed could produce a significant amount of heat at the interface [18, 24, 25]. The significantly large amount of heat can locally melt the interface and a following event of a rapid cooling could create the in situ development of intermediate layer that contains the porous structure. Based on our previous study [18], related to various sources of heating that could influence the interfacial kinematics, the Joule effect is not a significant contributor to the interfacial heating. This is mainly due to the so called skin effect that heats the outer of the tube while the interface could only heat to the maximum of approximately 50°C due to the Joule effect. Therefore, the interfacial heating and cooling rates at the onset due to the Joule effect is negligible in comparison with other kinematic heating contribution from thermo-mechanical effects. Therefore, this study was particularly dedicated to investigate the contribution of rapid heating and cooling, with the interfacial pressure of the molten pool and those results predominantly supports the development of porous inner architecture.

Some potential characteristics of the porous structure formed at an aluminum/aluminum interface during an EMPW are shown in Fig. 1. The welding tests were carried out on a tubular assembly with an overlap configuration using the electrical pulse generator of PULSAR MPW 25 kJ – 9 kV. The experimental test case is conducted with an input voltage of 7.5 kV with 1.5 mm initial gap between the flyer tube and rod, made of aluminum alloy AA6061 – T6 as received. The generator transforms the low-voltage power supply into a high voltage, and that also contains a capacitor bank with the total capacitance of 690 µF. The electric discharge through an inductive multi-turn coil generates large Lorentz force on the tube that causes the plastic deformation and subsequent collision of the flyer tube onto the fixed inner part. The discharge pulse frequency of 10 kHz was measured using a Rogowski probe inside the working area. The inductive multi turn coil used here, is composed of 3 turns and a field shaper is used to concentrate the magnetic field in the working section, which has 15 mm length and 27 mm in diameter. Additional details of the process description could be found elsewhere [7]. Porous structures observed at the Al/Al interfaces for the test case reveal a pocketed and layered appearance in the localized region of the interface (Fig 1). Typical pore sizes vary between few hundred nanometers to approximately less than 2 µm. It is also clearly noticeable that the inner architecture of the porous zone follows a wavy pattern and spreads for approximately 25 µm thickness along the interface. Moreover, there exists a few micro cracks within the porous zone, and they were bounded within the zone itself, also supports the hypothesis of the expansion of the pores during its coalescence and growth within the molten intermediate phase.

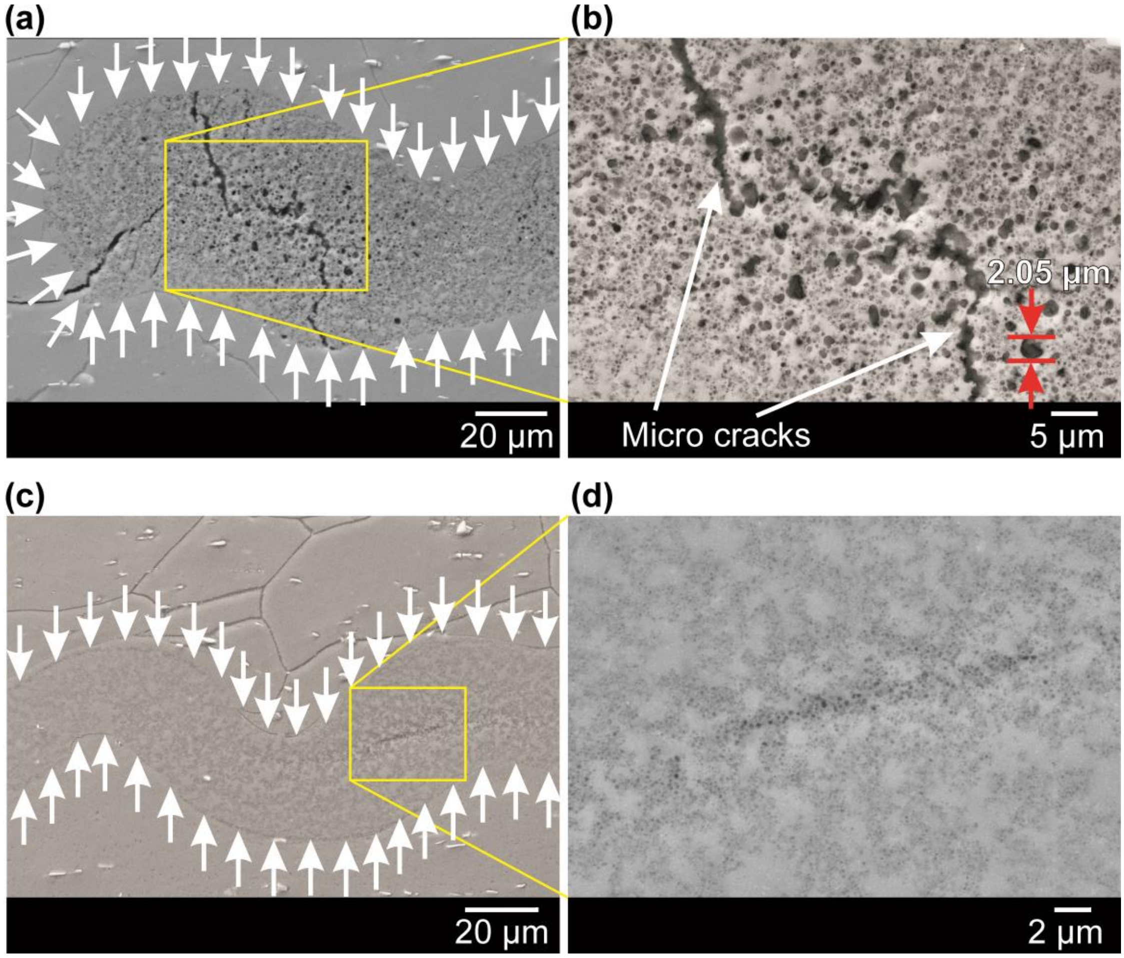

Fig.1. Potential features of porous structures observed at the Al/Al interface obtained from an EMPW process with the processing parameters of 7.5 kV input voltage and 1.5 mm initial air gap between the flyer and the rod.

Even though, these SEM observations clearly show the formation of porous structure at the interface, governing physical phenomena of the porous structure formation is still unclear, thereby, it motivates further investigations. Rice and Tracey have been pioneered in developing void growth model, where the rate of growth depends on the hydrostatic stress, von Mises norm of the Cauchy stress tensor (the equivalent stress) and equivalent plastic strain [28, 29]. The void growth happened during the EMPW is also attributable to the spherical void growth phenomena and could be treated as similar to that of a ductile problem in continuum plasticity [28]. Later various researchers investigated potential void growth behaviors and coalescence phenomena of porous structure, more details could be found elsewhere, e.g. [29, 30]. However, the interpretation of this situation as a valuable cause of sub micron sized pores formation becomes tricky due to the lack of phenomenological understandings, particularly for such small sized porosity. Therefore, a thermo-mechanical numerical simulation is proposed to investigate the porous structure formation.

The thermo-mechanical numerical simulation was performed in Abaqus package using Eulerian simulation technique. Please refer to our previous publication for full detail of the Eulerian method and its input material parameters [31]. The simulation was conducted for the case of 1.5 mm initial air gap with 7.5 kV input voltage; to predict the high heating and cooling rates, interfacial pressure, and strain components for those interfacial elements where the formation of porous structure occurs. The velocity input used in the model was obtained using another separate electromagnetic-thermomechanical coupled simulation using LS-Dyna and the data following the trend described in the EQ 1. The "coefficient of determination" (R^2) for the linear interpolation is 98.31%.

$$|V_y| = -24770|x| + 432 \;\; ; \forall x \in [0,0.0075] \tag{1}$$

where, $|V_y|$ (in ms^{-1}) is the magnitude of impact velocity along the y direction, and x (in m) is the distance from the top edge of the flyer (according to the coordinate system shown in Fig. 2).

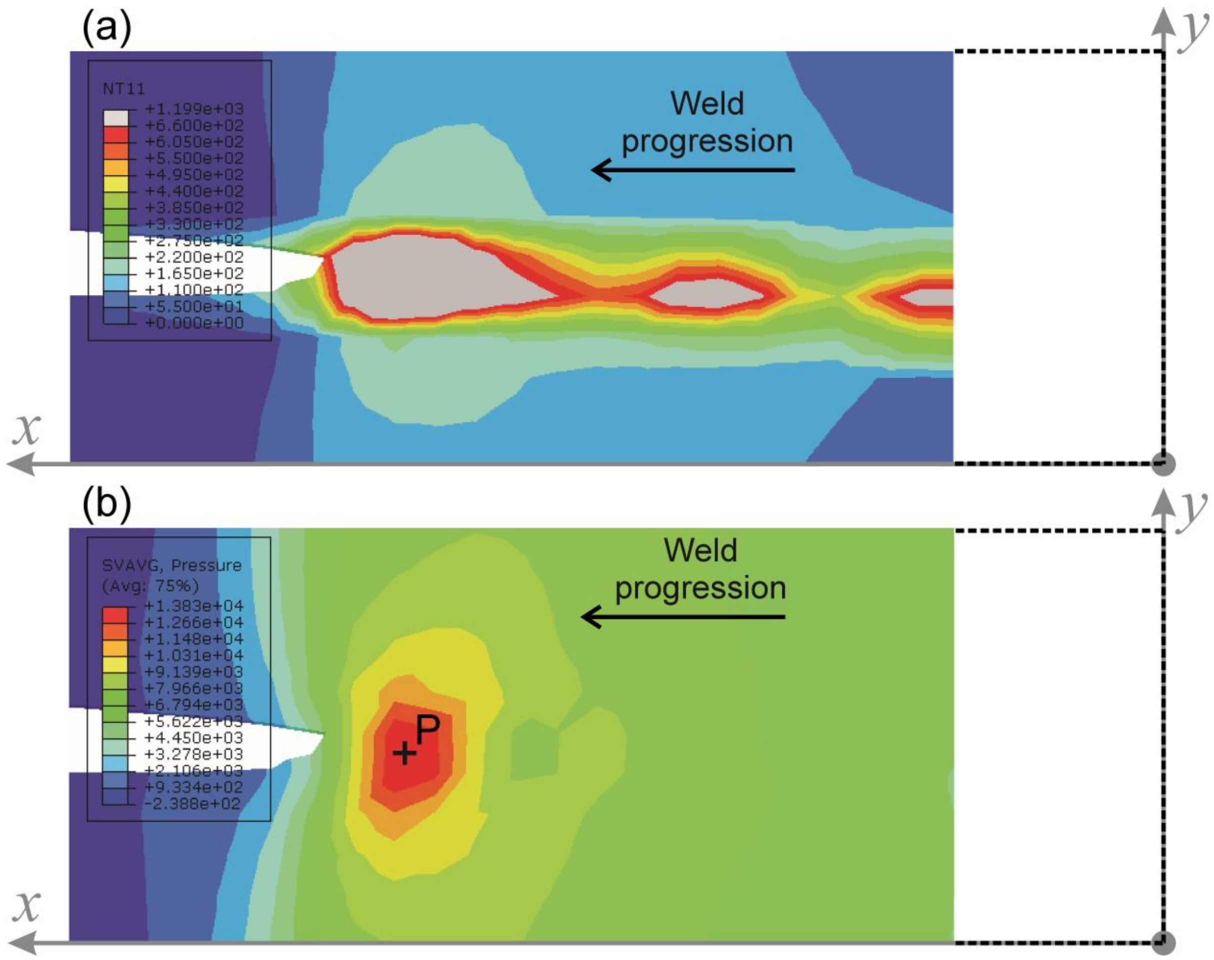

Fig. 2. A snap shot of temperature distribution in °C during the welding progress at the joint obtained from the thermo-mechanical simulation in (a), a snap shot of pressure (SVAVG) distribution in MPa, computed as a volume fraction weighted average of all materials within the elements during the Eulerian simulation in (b). The time dependent changes in temperature, pressure and strain components of the point "P" (indicated in b) is plotted in Fig. 3.

The thermo-mechanical numerical simulation allows predicting the interfacial heating effect with the rapid pressure changes that evidence the favorable condition for the pore nucleation as a result of extremely high localized temperature that induces melting of the interfacial material. Fig. 2a shows the temperature distribution of the interface region with the change in temperature of more than 660°C to 1200°C, in agreement with the shape and site occurrence of the porous intermediate phases (Fig 1). Pressure (SVAVG), computed as a volume fraction weighted average of all materials within the elements during the Eulerian simulation, and is shown in Fig. 2b. The advancing impact point (with time) clearly indicates the high pressure region, while the localized high pressure regions behind the impact point are eliminated and reached to a medium pressure level of ~ 680 MPa (Fig. 2b). Moreover, in order to understand the contribution of heating, cooling and interfacial pressure during the formation of the porous structure, the time dependant evaluations of the rapid heating and cooling, interfacial pressure and strain components of a particular interfacial point "P" (marked in Fig. 2b) are further investigated.

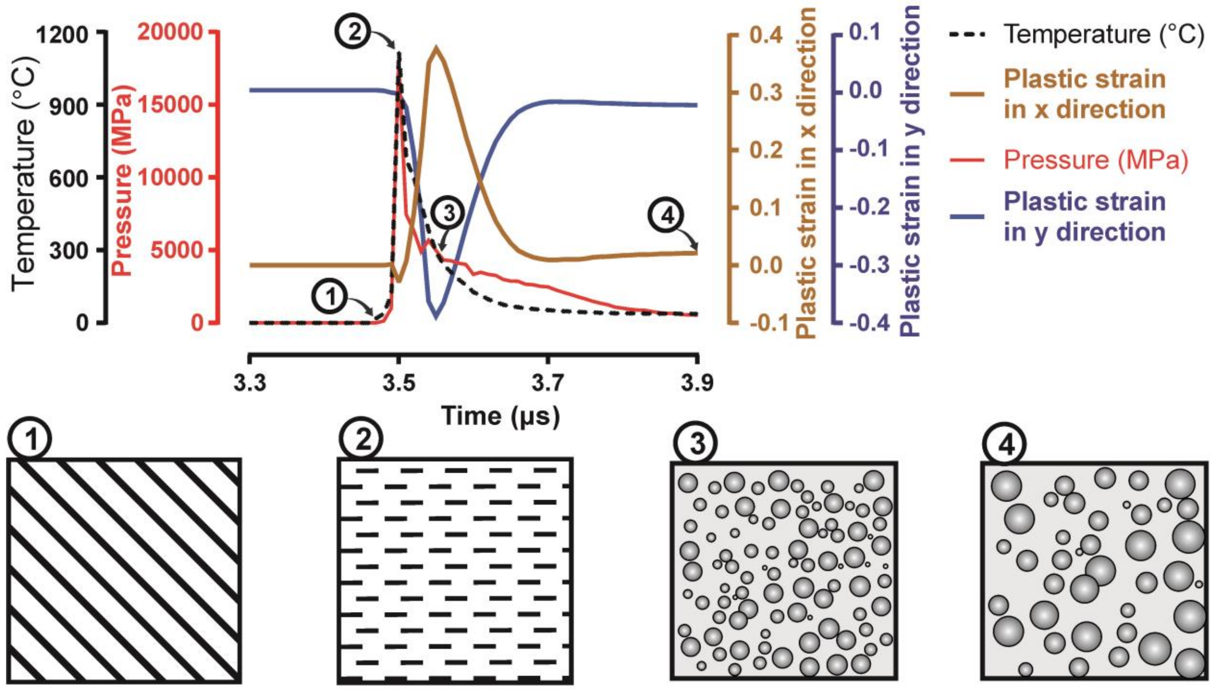

Fig. 3. Changes in Temperature, pressure and strain components of the point "P" (please refer to Fig. 2b) at the interface is plotted against time, and typical stages and porous structure formation are illustrated in the insets of 1-4; (1) interface material at its solid state before the onset of collision, (2) interface material changed to molten liquid state after the rapid heating, (3) nucleated porous structure and (4) continuous coalescence and growth until they become solidified structure when the temperature decreases.

As shown in Fig. 3., during the collision, the interface experiences a significant rise in temperature with an ultra high heating rate of approximately 10^9 °Cs^{-1}, when the interface is melted (stage 1 to 2) while the temperature continues to grow until it reaches the maximum value (stage 2). Then, a cooling (stage 2 to 4) occurs and the melted zone becomes solidified (stage 4). During the period of melted stage, typically a point of melting until the solidification, there is a large plastic strain with considerably high pressure (approximately 5000 MPa at Stage 3). According to the theory of Rice and Tracey [28], these conditions are favorable for the growth of voids. At the same time the volume of the material is subjected to a sudden temperature increase, and subsequently followed by a rapid cooling under isochoric condition (constant volume), when cavities are formed to maintain the conservation of the total volume in the material. The circular nature of the pores at the interface emphasizes that the formation mainly occurs due to an expansion that may also promoted by the depressurization that occurs during the cooling (stage 2 to 4), before and after the solidification. Thus, the porous structure is able to appear within the molten liquid due to this expansion with a benefic effect of the depressurization.

Mainly from stage 3 to 4, contraction/shrinkage occurs during the cooling that could also facilitate the growth and coalescence of pores within the confined volume. At the solid state, i.e. from stage 3, the shrinkage/expansion of the solidified porous structure may produce the micro cracks within the porous zones. These predictions are also attributable to dissimilar combination of materials, e.g. Al/Fe, where an interfacial amorphization has been evidenced due to similar rapid heating, melting and rapid cooling phenomena [21, 22].

In summary, the nucleation and growth of the pores may result from the cavitation phenomena by vaporization, surface tension of the fluid or confined bubbling. Under the high pressure condition the vaporization of aluminum can occur at lower temperature than that of the vaporization temperature under the ambient conditions. The coalescence phenomenon explains the spherical shape of the porosity and the formation of the open pores as a result of a radial growth of vaporized pores, or a fast expansion of the melted zone. The fast cooling of the intermediate phase freezes the porosity while the heat confined within the thin layer quickly diffuses toward the base metals that have a wide area and lower temperature than that of the interface. These consecutive phenomena potentially lead to the formation of porous interface. The coupled thermo-mechanical numerical simulation supports the local temperature increase at the interface and predicts the rapid heating and cooling rates of the intermediate phases, combined with a rapid expansion as a result of depressurization. The simulation results also corroborate the experimental observations in terms of the location and the shape of the melted zone. The overall investigation shows a method to produce a porous interface containing sub-micron to few micron sized pores that merits to be further investigated.

Acknowledgements

Authors acknowledge the funding support for the MSIM project from "Région Picardie" and for COILTIM project from "Région Picardie" and "Le fonds européen de développement économique et régional (FEDER)". Authors also thank "Plateforme Innovaltech" for its collaboration.

References

[1] M. Qu, Y. Wu, V. Srinivasan, A. Gouldstone, Observations of nanoporous foam arising from impact and rapid solidification of molten Ni droplets, Appl. Phys. Lett. 90(25) (2007) 254101.

[2] J.R. Johnson, G. Taber, A. Vivek, Y. Zhang, S. Golowin, K. Banik, G.K. Fenton, G.S. Daehn, Coupling Experiment and Simulation in Electromagnetic Forming Using Photon Doppler Velocimetry, Steel Res. Int. 80(5) (2009) 359-365.

[3] Y. Zhang, S. Babu, G. Daehn, Interfacial ultrafine-grained structures on aluminum alloy 6061 joint and copper alloy 110 joint fabricated by magnetic pulse welding, J. Mater. Sci. 45(17) (2010) 4645-4651.

[4] K. Lee, S. Kumai, T. Arai, T. Aizawa, Interfacial microstructure and strength of steel/aluminum alloy lap joint fabricated by magnetic pressure seam welding, Mater. Sci. Eng., A 471(1–2) (2007) 95-101.

[5] Z. Xu, J. Cui, H. Yu, C. Li, Research on the impact velocity of magnetic impulse welding of pipe fitting, Mater. Des. 49 (2013) 736-745.

[6] R.N. Raoelison, T. Sapanathan, N. Buiron, M. Rachik, Magnetic pulse welding of Al/Al and Al/Cu metal pairs: Consequences of the dissimilar combination on the interfacial behavior during the welding process, J. Manuf. Process. 20, Part 1 (2015) 112-127.

[7] R. Raoelison, N. Buiron, M. Rachik, D. Haye, G. Franz, M. Habak, Study of the elaboration of a practical weldability window in magnetic pulse welding, J. Mater. Process. Technol. 213(8) (2013) 1348-1354.

[8] R. Raoelison, D. Racine, Z. Zhang, N. Buiron, D. Marceau, M. Rachik, Magnetic pulse welding: Interface of Al/Cu joint and investigation of intermetallic formation effect on the weld features, J. Manuf. Process. 16(4) (2014) 427-434.

[9] H. Yu, Z. Xu, Z. Fan, Z. Zhao, C. Li, Mechanical property and microstructure of aluminum alloy-steel tubes joint by magnetic pulse welding, Mater. Sci. Eng., A 561(0) (2013) 259-265.

[10] H. Yu, Z. Xu, H. Jiang, Z. Zhao, C. Li, Magnetic pulse joining of aluminum alloy–carbon steel tubes, Trans. Nonferrous Met. Soc. China 22, Supplement 2(0) (2012) s548-s552.

[11] X. Wu, J. Shang, An investigation of magnetic pulse welding of Al/Cu and interface characterization, Journal of Manufacturing Science and Engineering 136(5) (2014) 051002.

[12] M. Marya, S. Marya, D. Priem, On the characteristics of electromagnetic welds between aluminium and other metals and alloys, Weld. World 49(5-6) (2005) 74-84.

[13] V. Shribman, Y. Livshitz, O. Gafri, Magnetic pulse welding and joining–a new tool for the automotive, SAE [Tech. Pap.] (2001) 3401-3408.

[14] J.Y. Shim, I.S. Kim, K.J. Lee, B.Y. Kang, Experimental and numerical analysis on aluminum/steel pipe using magnetic pulse welding, Met. Mater. Int. 17(6) (2011) 957-961.

[15] V. Shribman, Magnetic Pulse welding for dissimilar and similar materials, 3rd International Conference on High Speed Forming, TU Dortmund, Dortmund, 2008, pp. 13-22.

[16] E. Uhlmann, A. Ziefle, Modelling pulse magnetic welding processes–an empirical approach, 4th International Conference on High Speed Forming, Columbus, Ohio, USA, 2010, pp. 108-116.

[17] A. Nassiri, G. Chini, A. Vivek, G. Daehn, B. Kinsey, Arbitrary Lagrangian–Eulerian finite element simulation and experimental investigation of wavy interfacial morphology during high velocity impact welding, Mater. Des. 88 (2015) 345-358.
[18] T. Sapanathan, K. Yang, D. Chernikov, R. Raoelison, V. Gluschenkov, N. Buiron, M. Rachik, Thermal Effect during Electromagnetic Pulse Welding Process, THERMEC 2016, Trans Tech Publications, Graz, 2016.
[19] A. Stern, V. Shribman, A. Ben-Artzy, M. Aizenshtein, Interface Phenomena and Bonding Mechanism in Magnetic Pulse Welding, J. Mater. Eng. Perform. 23(10) (2014) 3449-3458.
[20] M. Geyer, S. Böhm, Influence of contact surface on weldability with electromagnetic pulses, IIW Denver Annual Assembly (2012).
[21] J. Li, Q. Yu, Z. Zhang, W. Xu, X. Sun, Formation mechanism for the nanoscale amorphous interface in pulse-welded Al/Fe bimetallic systems, Appl. Phys. Lett. 108(20) (2016) 201606.
[22] Z. Fan, H. Yu, C. Li, Interface and grain-boundary amorphization in the Al/Fe bimetallic system during pulsed-magnetic-driven impact, Scr. Mater. 110 (2016) 14-18.
[23] S. Sharafiev, C. Pabst, M.F. Wagner, P. Groche, Microstructural characterisation of interfaces in magnetic pulse welded aluminum/aluminum joints, 18th Chemnitz Seminar on Materials Engineering, IOP Publishing, Chemnitz, 2016, pp. 1-5.
[24] C. Pabst, P. Groche, Electromagnetic Pulse Welding: Process Insights by High Speed Imaging and Numerical Simulation, 6th International Conference on High Speed Forming, Institut für Umformtechnik - Technische Universität Dortmund, South Korea, 2014, pp. 77-88.
[25] P. Groche, C. Pabst, Numerical simulation of impact welding processes with LS-DYNA, 10th European LS-DYNA Conference, Würzburg, Germany, 2015.
[26] S. Kakizaki, M. Watanabe, S. Kumai, Simulation and experimental analysis of metal jet emission and weld interface morphology in impact welding, Mater. Trans. 52(5) (2011) 1003-1008.
[27] A. Stern, O. Becher, M. Nahmany, D. Ashkenazi, V. Shribman, Jet Composition in Magnetic Pulse Welding: Al-Al and Al-Mg Couples MPW jet phenomena were investigated and jet material cornposition for similar Al alloys and two samples of dissimilar Al-Mg alloy couples were observed, Weld. J. (Miami, FL, U. S.) 94(8) (2015) 257S-264S.
[28] J.R. Rice, D.M. Tracey, On the ductile enlargement of voids in triaxial stress fields, J. Mech. Phys. Solids 17(3) (1969) 201-217.
[29] T. Pardoen, F. Delannay, Assessment of void growth models from porosity measurements in cold-drawn copper bars, Metall. Mater. Trans. A 29(7) (1998) 1895-1909.
[30] T. Pardoen, I. Doghri, F. Delannay, Experimental and numerical comparison of void growth models and void coalescence criteria for the prediction of ductile fracture in copper bars, Acta Mater. 46(2) (1998) 541-552.
[31] T. Sapanathan, R.N. Raoelison, E. Padayodi, N. Buiron, M. Rachik, Depiction of interfacial characteristic changes during impact welding using computational methods: Comparison between Arbitrary Lagrangian - Eulerian and Eulerian simulations, Mater. Des. 102 (2016) 303-312.